

Proton-Induced, Reversible Interconversion of a μ -1,2-Peroxo and a μ -1,1-Hydroperoxo Dicopper(II) Complex

Nicole Kindermann, Sebastian Dechert, Serhiy Demeshko, and Franc Meyer*

Institut für Anorganische Chemie, Georg-August-Universität Göttingen, Tammannstraße 4, 37077 Göttingen, Germany

S Supporting Information

ABSTRACT: The μ -1,2-peroxo dicopper(II) complex (**2**) of a compartmental bis(tetradentate) pyrazolate-based ligand is shown to convert, upon protonation, to the corresponding μ -1,1-hydroperoxo dicopper(II) complex (**3**). The transformation is cleanly reversed with base, and an apparent $pK_a = 22.2 \pm 0.3$ for the Cu_2OOH unit in MeCN has been determined. The unprecedented stability of **3** ($t_{1/2} = 9$ h in nitrile solvents at room temperature, giving the hydroxo-bridged dicopper complex) has allowed for its structural characterization by X-ray diffraction. While the O–O bond length (1.462(3) Å) barely changes upon protonation from **2** to **3**, the O–O stretching frequency is much higher in the hydroperoxo complex **3** (860 cm^{-1}). **3** mediates $2e^-$ oxo transfer to the nucleophilic substrate PPh_3 but is not activated for H-atom abstraction.

Copper–dioxygen complexes are of considerable interest in bioinorganic chemistry, since they provide a thorough understanding of reactive intermediates that occur in the parent enzymes' copper active sites.¹ This insight is beneficial also for the rational design of homogeneous catalytic systems that can mediate reactions beyond those originally accomplished by the metalloproteins.² In particular, the bioinspired use of molecular oxygen for oxidation and oxygenation of C–H bonds has become of fundamental importance for scenarios toward a more sustainable generation of chemical feedstocks and fuels.³ Identifying the key metal (M)–dioxygen (O_2) intermediates and elucidating their (electronic) structures and functional principles, including their protonation and redox events, are thus important goals.

Compartmental pyrazolate/triazacyclononane (pz/tacn) hybrid ligands HL^{me} and HL^{et} have recently allowed for the isolation of the first dicopper peroxo complex with a *cis*- μ -1,2 binding mode (**1**; Figure 1)⁴ and of an unprecedented *trans*- μ -

1,2-peroxo dicopper(II) complex (**2**) having a triplet ground state.⁵ These dicopper/ O_2 intermediates represent snapshots of the initial stages of the O_2 binding trajectory in type III copper proteins such as hemocyanin (Hc) and tyrosinase (Ty).⁶ Beneficial characteristics of the pz/tacn ligand scaffolds are the high stability they impart to the bimetallic core and the high degree of preorganization that allows for adjusting the M···M separation, and hence for controlling the binding mode of exogenous ligands (e.g., peroxide) within the bimetallic pocket.⁷ A unique feature in **1** was the side-on interaction of the bridging peroxo with a sodium cation, both in solution and in the solid state;⁴ interaction with Lewis acids such as Na^+ surprisingly was not observed for closely related **2**. We have now investigated whether **2** would react with the simplest and smallest Lewis acid, H^+ . From the work of Karlin et al., it is known that *trans*- μ -1,2-peroxo dicopper(II) complexes can transform, upon protonation, to the corresponding 1,1- μ -hydroperoxo complexes;⁸ these interesting species were found to have a rich substrate oxidative chemistry.⁹ For some time, a Cu-bridging hydroperoxo was suggested as a potential intermediate during O_2 reduction at the trinuclear active site of multicopper oxidases such as laccase,¹⁰ and, more recently, μ -1,1-hydroperoxo dicopper(II) species have been implicated as crucial intermediates in the catalytic $2e^-/2H^+$ and $4e^-/4H^+$ reductions of O_2 mediated by dinuclear copper complexes.¹¹ Protonation of *trans*- μ -1,2-peroxo dicopper(II) species to give the μ -1,1-hydroperoxo congener was indeed shown to represent a key step in the selective $2e^- O_2$ reduction process. However, protonation of dicopper peroxo complexes has so far been found irreversible, and most of the reported species suffer from thermal instability.¹² Furthermore, there is a distinct lack of crystallographic data for μ -1,1-hydroperoxo dicopper complexes in the literature, since only one example can be found, and in that case detailed structural analysis was prevented by severe ligand disorder of the complex core.¹³ In this Communication, making use of the pz/tacn ligand scaffold, we now present the full characterization of a μ -1,1-hydroperoxo dicopper(II) complex, including unambiguous determination of its metric parameters, together with reversibility studies of proton binding that allow for estimating the hydroperoxo pK_a .

Dicopper(I) complex $[L^{et}Cu_2](BPh_4)$ readily reacts with O_2 to form a deep purple solution. This O_2 adduct was shown to be a μ -1,2 dicopper(II) peroxo complex (**2**) with a Cu–O–O–Cu torsion close to 90° induced by ligand design, representing the first member of the dicopper(II) peroxo family with a triplet ground state (see Figure 1).⁵ When **2** was reacted with 2,6-

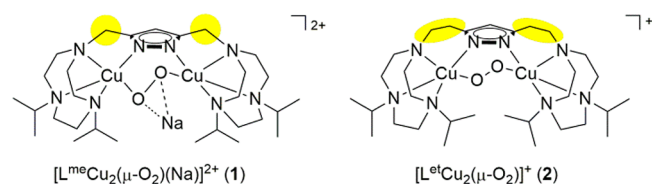


Figure 1. Previously described dicopper oxygen adducts **1** and **2** based on pz/tacn scaffolds,^{4,5} with differences in the ligand systems L^{me} and L^{et} highlighted in yellow.

Received: April 27, 2015

Published: June 10, 2015

lutidinium triflate (HLuOTf), the characteristic charge-transfer (CT) absorption band of **2** at 506 nm ($\epsilon = 4800 \text{ M}^{-1} \text{ cm}^{-1}$) disappeared, whereas a strong new absorption at 416 nm grew in, with a clean isosbestic point at 453 nm (Figure 2). Trans-

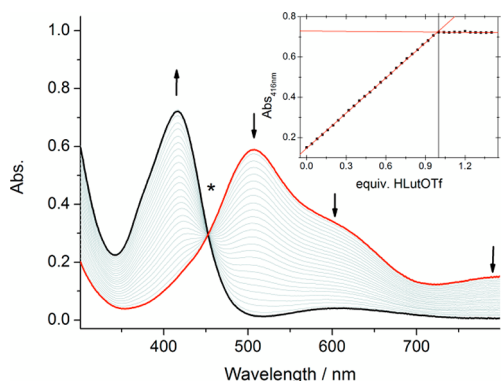


Figure 2. Stepwise protonation of the $\{\text{Cu}_2\text{O}_2\}$ species **2** (red spectrum) with HLuOTf at -20°C in propionitrile (0.125 mM), monitored by UV/vis absorption spectroscopy (1 cm path length). Changes in the spectrum are indicated by black arrows; the asterisk marks the isosbestic point at 453 nm. Inset: increase of the absorption at 416 nm depending on the number of equivalents of HLuOTf added.

formation was complete after 1 equiv of acid was added, and the product **3** was stable in the presence of excess HLuOTf. Based on the distinct optical transition^{8,9,12b} and the observed stoichiometry, the newly formed Cu_2/O_2 species **3** was assigned to be a μ -1,1-hydroperoxo dicopper(II) complex. Its intense absorption at 416 nm ($\epsilon = 5700 \text{ M}^{-1} \text{ cm}^{-1}$) with a weaker shoulder at 373 nm ($\epsilon = 3300 \text{ M}^{-1} \text{ cm}^{-1}$) is typical for hydroperoxo ligand-to-metal charge transfer (LMCT), whereas the weak and broad band at 605 nm ($\epsilon = 300 \text{ M}^{-1} \text{ cm}^{-1}$) originates from a ligand field transition.^{12b} The relatively high intensity of the LMCT bands likely reflects significant covalency between the hydroperoxo ligand and Cu(II), and the position of the d–d transition indicates a roughly square-planar Cu(II) coordination environment.¹⁴

The exceptional stability of **3** allowed for isolation of bulk material. To this end the dicopper(I) complex, dissolved in propionitrile, was first treated with O_2 at ambient temperature to obtain peroxo complex **2**, followed by the addition of HLuOTf. An immediate color change to dark green indicated hydroperoxo formation. Single crystals of **3** were grown from propionitrile solutions layered with diethyl ether between -20 and -30°C and were analyzed by X-ray diffraction (XRD). Figure 3 shows a pictorial representation of the cation of **3**; atom distances and bond angles can be found in the Supporting Information (SI), Tables S2 and S3. As anticipated, the core structure of **3** consists of two Cu(II) ions in a more or less distorted square-pyramidal environment ($\tau = 0.397$ and 0.035),¹⁵ hosted in the $\{\text{N}_4\}$ binding pockets of the pz/tacn hybrid ligand and bridged by an end-on bound hydroperoxo moiety.

Transformation of **2** to **3** requires a rearrangement of the μ -1,2 peroxo ligand to the μ -1,1 coordination mode. Upon protonation and rearrangement, the O–O bond length hardly changes (1.460(2) Å in **2** vs 1.462(3) Å in **3**), whereas the distance between the Cu-atoms shrinks from 3.677 to 3.533 Å. As observed in the previously reported pyrazolate-based dicopper(II)/ O_2 adducts **1** and **2**,^{4,5} the Cu–N bonds to the anionic pyrazolate and the Cu–O bonds are significantly shorter (<2.0 Å) than the Cu–N bonds involving the tacn macrocycle. The

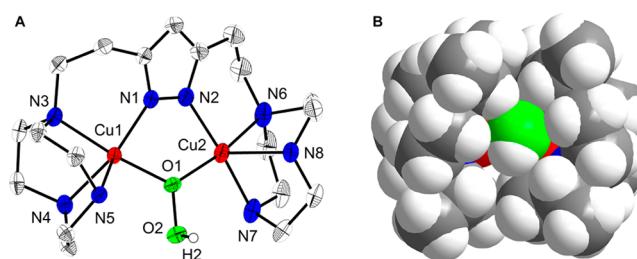


Figure 3. (A) Molecular structure of the cation of **3** with corresponding partial labeling scheme; thermal displacement ellipsoids drawn at 50%. BPh_4^- counterions, H-atoms (except OOH), co-crystallized solvent molecules, and isopropyl substituents at N4, N5, N7, and N8 have been omitted for clarity. (B) Space-filling representation of the complete cationic portion of **3**, viewed from the front along the O–O axis.

local z -axes in **3** are rendered by the Cu1–N5 and the Cu2–N8 vectors, respectively, for which the longest bonds (2.303(3) and 2.340(3) Å) are indicative. The high quality of the XRD data made it possible to locate the H-atom of the hydroperoxo moiety in the electron density map. It points toward a triflate anion that was found in close proximity to the complex core ($d(\text{O}2\cdots\text{O}^{\text{OTf}}) = 2.79$ Å), suggesting the presence of a O–H \cdots O hydrogen bond that likely contributes to the high stability of **3**. Indeed, the only other example of a crystalline μ -1,1-hydroperoxo dicopper(II) complex also exhibits a H-bond, in that case to a close-by dangling N-atom of the ligand.¹³ However, reliable assignment of structural parameters in that previously reported dicopper hydroperoxo complex was hampered by severe disorder in the complex core. The hydroperoxo OOH plane in **3** is roughly orthogonal to the Cu1–O–Cu2 plane (dihedral angle between the OOH and CuOCu planes, 83.5°). This allows for efficient interaction of the stabilized π^*_{\perp} , which is orthogonal to the OOH plane and mostly localized on the Cu-bound O $^{\alpha}$ -atom of the hydroperoxo unit, with the local Cu $d_{x^2-y^2}$ orbitals (from DFT, see SI, Figure S6).^{12b} It should be noted that Cu–O covalency, judged on the intensity of the (hydro)peroxo π^* -to-Cu CT bands, is low in **2** compared to *trans*- μ -1,2-dicopper(II) peroxo complexes, but is similar in **2** and **3**.

Rearrangement of the peroxo bridge on going from **2** to **3** is also reflected in the magnetic ground state of the resulting complexes. The Cu–O–O–Cu torsion angle found in **2** (104°) caused the so far unique situation of ferromagnetic coupling between the two Cu(II) centers and an $S = 1$ ground state because of almost vanishing overlap of the magnetic orbitals.⁵ In contrast, rearrangement of the μ -1,2-peroxo ligand to the μ -1,1 mode turns on strong superexchange between the Cu(II) ions, mediated by the monoatomic end-on hydroperoxo bridge. Hence, the ground state becomes a greatly stabilized singlet ($S = 0$) as the two Cu(II) ions are now strongly antiferromagnetically coupled ($J = -538 \text{ cm}^{-1}$ based on SQUID data; see SI for details).

Resonance Raman data of solutions of $3[^{16}\text{O}_2]$ and $3[^{18}\text{O}_2]$ in MeCN (excitation at 457 nm) revealed only one signal sensitive to isotopic labeling, namely a peak at 860 cm^{-1} that shifted to 814 cm^{-1} when natural abundance O_2 was exchanged against $^{18}\text{O}_2$ ($\Delta^{16}\text{O}_2-^{18}\text{O}_2 = -46 \text{ cm}^{-1}$; Figure 4). Similar values were found in Raman measurements of solid material, though the peak for the $^{16}\text{O}-^{16}\text{O}$ vibration was hidden by other resonances caused by the BPh_4^- anion (see SI for a detailed description). In contrast to the O–O stretch, no peak originating from Cu–O vibrations could be detected, which might be due to the poor signal-to-noise ratio of the Raman spectrum below 600 cm^{-1} . Although no

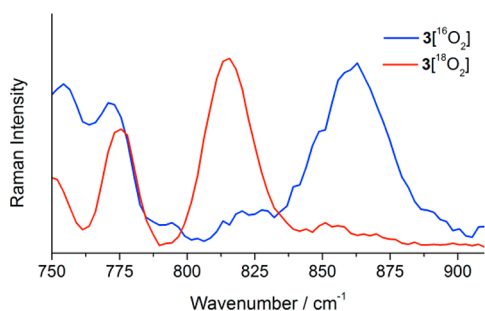


Figure 4. Resonance Raman spectra of **3** (BPh_4^- as counterion) at room temperature in acetonitrile (natural abundance O_2 in blue, $^{18}\text{O}_2$ labeled in red); excitation wavelength, 457 nm.

significant change in the O–O bond length was observed upon protonation, the O–O stretching frequency in **2** is much lower at 803 cm^{-1} . According to Badger's rule, a similar bond length indicates a similar force constant and is thus commonly associated with similar frequencies for the respective bond vibration.¹⁶ Apparently, this is not the case for peroxo complex **2** and its protonated congener **3**. Previous work by Solomon et al. on diiron and dicopper (hydro)peroxo complexes suggested significant mechanical coupling between $\nu(\text{Cu}-\text{O})$ and $\nu(\text{O}-\text{O})$ in this case, depending on the M–O–O angles.^{12b,17} For **3**, these angles are 114° and 120° , which would indeed lead to mechanical coupling between both vibrations and thus explain the unexpected shift of $\nu(\text{O}-\text{O})$ to higher energy. From IR data (SI, Figure S4), the OO–H vibration could be located at 3394 cm^{-1} , shifting to 3383 cm^{-1} upon $^{18}\text{O}_2$ substitution ($\Delta^{16}\text{O}_2-^{18}\text{O}_2 = -11\text{ cm}^{-1}$), and to 2511 cm^{-1} in samples crystallized in the presence of CH_3OD . The observed frequencies for all vibrations associated with the hydroperoxo bridge are in good agreement with other reported examples of μ -1,1-hydroperoxo dicopper(II) complexes.^{8,9,12b} It should also be noted that the O–O stretching frequency of **3** is similar to that of H_2O_2 (877 cm^{-1}).¹⁸

Protonation of **2** has also been studied by means of UV/vis stopped-flow experiments to see whether short-lived intermediates of the protonation/rearrangement scenario, such as a side-on protonated species akin to the Na^+ complex **1** (Figure 1), could be characterized. To this end, 1 equiv of HLutOTf was rapidly mixed with **2** in propionitrile (SI, Figures S16 and S17). However, even at the lowest temperature attainable with our instrument ($-75\text{ }^\circ\text{C}$), most of the $\{\text{Cu}_2\text{O}_2\}$ species **2** was already converted into its protonated analogue **3** after 12 ms, and no clean intermediate could be detected. From the data, an approximate second-order rate constant of $(5.8 \pm 1.2) \times 10^5\text{ L}\cdot\text{mol}^{-1}\cdot\text{s}^{-1}$ at $-75\text{ }^\circ\text{C}$ could be derived for the peroxo-to-hydroperoxo transformation.

Reversibility of the protonation and rearrangement was then studied in more detail through back-titration experiments with strong organic bases. Interestingly, addition of 1,8-diazabicycloundec-7-ene (DBU; $\text{p}K_a = 24.3$ in MeCN)¹⁹ to **3** indeed resulted in the recovery of peroxo complex **2**. Following the reaction by UV/vis spectroscopy, it was found that $\sim 95\%$ of the initial absorption of **2** could be restored at $-20\text{ }^\circ\text{C}$. This contrasts previously reported μ -1,1-hydroperoxo dicopper(II) complexes, for which no deprotonation could be observed without decomposition. Various bases were then screened to determine the apparent $\text{p}K_a$ of the hydroperoxo ligand in **3**.²⁰ 1,1,3,3-Tetramethylguanidine (TMG; $\text{p}K_a = 23.3$ in MeCN)²¹ was found to give a proper equilibrium, and monitoring back-titration

with TMG by means of absorption spectroscopy gave an apparent $\text{p}K_a = 22.2 \pm 0.3$ for **3** in MeCN according to mass balance. Details on the fit, generic titration data, and plots to derive $\text{p}K_a(\mathbf{3})$ can be found in the SI, Figures S11–S13. Considering that the $\text{p}K_a$ of TMG in water (~ 13) is ~ 1 unit higher than that of H_2O_2 (11.8), it can be estimated that the Cu_2OOH motif in **3** has an acidity roughly similar to that of H_2O_2 .

The μ -1,1-hydroperoxo dicopper(II) complex **3** proved exceptionally stable, exhibiting a half-life time of $\sim 9\text{ h}$ in EtCN, MeCN, or MeCN- d_3 solutions at room temperature (see Figure 5). Even an excess of acid did not lead to an increased

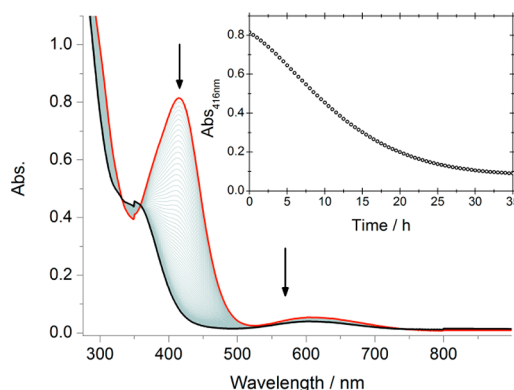
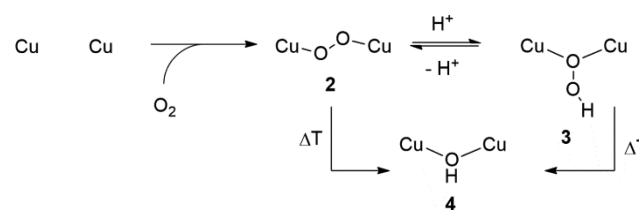


Figure 5. Thermal decay of **3** in EtCN (red line), followed spectrophotometrically at room temperature. Arrows indicate development of the bands. Inset: time trace for the absorption at 416 nm over the course of 35 h.

decay rate; i.e., release of H_2O_2 under these conditions does not occur. The yellow-greenish solution of **3** gradually turns light blue upon standing, but in contrast to other reported examples of dicopper(II) hydroperoxo complexes,^{8a,c,9a,12a,13,22} no self-oxidized ligand fragments or products from solvent oxidation could be detected. In this case, the only decay product isolated so far was shown to be the hydroxo-bridged $[\text{L}^{\text{Et}}\text{Cu}_2(\text{OH})](\text{BPh}_4)_2$ (**4**, together with its triflate analogue), which was also observed in the thermal decay of **2**, based on X-ray crystallography, ESI-MS data, and UV/vis features ($\lambda_{\text{max}} = 356\text{ nm}$ for LMCT, $\lambda_{\text{max}} = 613\text{ nm}$ for d–d transition).⁵ In contrast to other reported examples of μ -1,1-hydroperoxo dicopper(II) complexes, **3** could not be regenerated when H_2O_2 (aqueous solution or urea adduct in MeCN) was added to solutions of hydroxo complex **4**. Furthermore, the actual decay mechanism of **3** to **4** might be complex, as apparent from the time trace of the band at 416 nm (Figure 5, inset), since no simple exponential decay could be used to fit the experimental curve. The reaction sequence of the system $[\text{L}^{\text{Et}}\text{Cu}_2]^+/\text{O}_2$ is summarized in Scheme 1.

Scheme 1. Reaction Sequence of Dinuclear Copper Complex $[\text{L}^{\text{Et}}\text{Cu}_2]^+$ with Dioxygen



Substrate oxidation ability was tested with in situ generated **3**. Whereas 1,4-cyclohexadiene or thioanisole did not lead to any significant increase in decay of **3** at room temperature, PPh₃ addition caused a faster depletion of characteristic UV/vis absorptions (see SI, Figure S14) compared to self-decay. Hence, this reaction was investigated more thoroughly by mixing of PPh₃ with crystalline **3** under inert conditions. ¹H and ³¹P NMR revealed triphenylphosphine oxide as the oxo transfer product, with an approximate yield of (94 ± 5)%, whereas the UV/vis spectrum showed characteristic absorptions of hydroxo-bridged compound **4**. These results are in line with previous findings that μ -1,1-hydroperoxy dicopper(II) complexes are electrophilic and are capable of 2e⁻ oxo transfer to readily oxidizable nucleophilic substrates such as PPh₃ but not activated for 1e⁻ oxidations via H-atom abstraction because of the high O–O bond strength.^{12b,17b} The reactivity of **3** may be further restricted by the limited accessibility of the hydroperoxy group, which is sterically shielded by the ligand scaffold, as evident from the space-filling model shown in Figure 2. This might also be the cause for the observed acid stability of **4**.

In summary, we were able to isolate a μ -1,1-hydroperoxy dicopper(II) complex that shows remarkable stability at ambient temperatures. This allowed for its comprehensive characterization, including its structure determination by XRD. Stopped-flow analysis showed the transformation of the μ -1,2-peroxy to the μ -1,1-hydroperoxy dicopper(II) complex upon protonation to be very fast, without detectable intermediate. Unprecedented reversibility of the protonation/deprotonation induced transformation was observed, and an apparent pK_a = 22.2 ± 0.3 for the Cu₂OOH unit in MeCN derived, showing that the acidities of the Cu₂OOH unit and H₂O₂ are similar. Because of its stability, **3** is a sluggish oxygen-atom-transfer reagent, and its reaction with PPh₃ is relatively slow. The new μ -1,1-hydroperoxy dicopper(II) complex **3** represents the first of its kind for which metric parameters could be unambiguously determined and compared with parameters of its corresponding base, the unprotonated parent peroxy congener. Interconversions between, and equilibria of, different Cu₂/O₂ species are emerging as an intriguing scenario for switching between various types of reactivity of these important intermediates,²³ and proton (or pH)-induced interconversions should be of particular biological relevance.

■ ASSOCIATED CONTENT

■ Supporting Information

Detailed synthetic procedures, crystallographic information, vibrational, NMR, and UV/vis spectroscopy; DFT calculations; magnetic data; substrate reactivity; and stopped-flow analysis. The Supporting Information is available free of charge on the ACS Publications website at DOI: 10.1021/jacs.5b04361.

■ AUTHOR INFORMATION

Corresponding Author

*franc.meyer@chemie.uni-goettingen.de

Notes

The authors declare no competing financial interest.

■ ACKNOWLEDGMENTS

Financial support from the Fonds der Chemischen Industrie, the Studienstiftung des deutschen Volkes (to N.K.), and the DFG (International Research Training Group 1422 “Metal Sites in

Biomolecules: Structures, Regulation and Mechanisms”) is gratefully acknowledged.

■ REFERENCES

- (1) (a) Jacobson, R. R.; Tyeklar, Z.; Farooq, A.; Karlin, K. D.; Liu, S.; Zubieta, J. *J. Am. Chem. Soc.* **1988**, *110*, 3690. (b) Kitajima, N.; Fujisawa, K.; Moro-oka, Y.; Toriumi, K. *J. Am. Chem. Soc.* **1989**, *111*, 8975. (c) Kitajima, N.; Moro-oka, Y. *Chem. Rev.* **1994**, *94*, 737. (d) Tolman, W. B. *Acc. Chem. Res.* **1997**, *30*, 227.
- (2) Que, L.; Tolman, W. B. *Nature* **2008**, *455*, 333.
- (3) Lee, J. Y.; Karlin, K. D. *Curr. Opin. Chem. Biol.* **2015**, *25*, 184.
- (4) Dalle, K. E.; Gruene, T.; Dechert, S.; Demeshko, S.; Meyer, F. *J. Am. Chem. Soc.* **2014**, *136*, 7428.
- (5) Kindermann, N.; Bill, E.; Dechert, S.; Demeshko, S.; Reijerse, E. J.; Meyer, F. *Angew. Chem., Int. Ed.* **2015**, *54*, 1738.
- (6) (a) Metz, M.; Solomon, E. I. *J. Am. Chem. Soc.* **2001**, *123*, 4938. (b) Solomon, E. I.; Sarangi, R.; Woertink, J. S.; Augustine, A. J.; Yoon, J.; Ghosh, S. *Acc. Chem. Res.* **2007**, *40*, 581. (c) Solomon, E. I.; Ginsbach, J. W.; Heppner, D. E.; Kieber-Emmons, M. T.; Kjaergaard, C. H.; Smeets, P. J.; Tian, L.; Woertink, J. S. *Faraday Discuss.* **2011**, *148*, 11.
- (7) (a) Klingele, J.; Meyer, F. *Coord. Chem. Rev.* **2009**, *253*, 2698. (b) Dalle, K.; Meyer, F. *Eur. J. Inorg. Chem.* **2015**, DOI: 10.1002/ejic.201500185.
- (8) (a) Karlin, K.; Cruse, R.; Gultneh, Y. *J. Chem. Soc., Chem. Commun.* **1987**, 599. (b) Karlin, K. D.; Ghosh, P.; Cruse, R. W.; Farooq, A.; Gultneh, Y.; Jacobson, R. R.; Blackburn, N. J.; Strange, R. W.; Zubieta, J. *J. Am. Chem. Soc.* **1988**, *110*, 6769. (c) Murthy, N. N.; Mahroof-Tahir, M.; Karlin, K. D. *Inorg. Chem.* **2001**, *40*, 628.
- (9) (a) Li, L.; Narducci Sarjeant, A. A.; Vance, M. A.; Zakharov, L. N.; Rheingold, A. L.; Solomon, E. I.; Karlin, K. D. *J. Am. Chem. Soc.* **2005**, *127*, 15360. (b) Li, L.; Narducci Sarjeant, A. A.; Karlin, K. D. *Inorg. Chem.* **2006**, *45*, 7160.
- (10) Rulisek, L.; Solomon, E. I.; Ryde, U. *Inorg. Chem.* **2005**, *44*, 5612.
- (11) (a) Fukuzumi, S.; Tahsini, L.; Lee, Y.-M.; Ohkubo, K.; Nam, W.; Karlin, K. D. *J. Am. Chem. Soc.* **2012**, *134*, 7025. (b) Das, D.; Lee, Y.-M.; Ohkubo, K.; Nam, W.; Karlin, K. D.; Fukuzumi, S. *J. Am. Chem. Soc.* **2013**, *135*, 4018.
- (12) (a) Mahroof-Tahir, M.; Murthy, N. N.; Karlin, K. D.; Blackburn, N. J.; Shaikh, S. N.; Zubieta, J. *Inorg. Chem.* **1992**, *31*, 3001. (b) Root, D. E.; Mahroof-Tahir, M.; Karlin, K. D.; Solomon, E. I. *Inorg. Chem.* **1998**, *37*, 4838.
- (13) Itoh, K.; Hayashi, H.; Furutachi, H.; Matsumoto, T.; Nagatomo, S.; Tosha, T.; Terada, S.; Fujinami, S.; Suzuki, M.; Kitagawa, T. *J. Am. Chem. Soc.* **2005**, *127*, 5212.
- (14) Hathaway, B. J. *Chem. Soc., Dalton Trans.* **1971**, 1196.
- (15) Addison, A. W.; Rao, T. N.; Reedijk, J.; van Rijn, J.; Verschoor, G. C. *J. Chem. Soc., Dalton Trans.* **1984**, 134.
- (16) Badger, R. M. *J. Chem. Phys.* **1934**, *2*, 128.
- (17) (a) Brunold, T. C.; Tamura, N.; Kitajima, N.; Moro-oka, Y.; Solomon, E. I. *J. Am. Chem. Soc.* **1998**, *120*, 5674. (b) Chen, P.; Fujisawa, K.; Solomon, E. I. *J. Am. Chem. Soc.* **2000**, *122*, 10177.
- (18) Giguère, P. A. *J. Chem. Phys.* **1950**, *18*, 88.
- (19) Kaljurand, I.; Kütt, A.; Sooväli, L.; Rodima, T.; Mäemets, V.; Leito, I.; Koppel, I. A. *J. Org. Chem.* **2005**, *70*, 1019.
- (20) To derive an apparent pK_a value for the hydroperoxide ligand, rearrangement of the ligand was ignored, and deprotonation was treated as a simple acid–base equilibrium (see SI for details).
- (21) Kovacevic, B.; Maksic, Z. B. *Org. Lett.* **2001**, *3*, 1523.
- (22) Sorrell, T. N.; Vankai, V. A. *Inorg. Chem.* **1990**, *29*, 1687.
- (23) (a) Halfen, J. A.; Mahapatra, S.; Wilkinson, E. C.; Kaderli, S.; Young, V. G., Jr.; Que, L., Jr.; Zuberbühler, A. D.; Tolman, W. B. *Science* **1996**, *271*, 1397. (b) Cahoy, J.; Holland, P. L.; Tolman, W. B. *Inorg. Chem.* **1999**, *38*, 2161. (c) Kieber-Emmons, M. T.; Ginsbach, J. W.; Wick, P. K.; Lucas, H. R.; Helton, M. E.; Lucchese, B.; Suzuki, M.; Zuberbühler, A. D.; Karlin, K. D.; Solomon, E. I. *Angew. Chem., Int. Ed.* **2014**, *53*, 4935.